

# TOPOGRAPHIC CORRECTION OF ZY-3 SATELLITE IMAGE AND ITS EFFECTS ON ESTIMATION OF SHRUBS LEAF BIOMASS IN MOUNTAINOUS AREA

Mingliang GAO<sup>a, b, c, \*</sup>, Wenji ZHAO<sup>a, b, c</sup>, Zhaoning GONG<sup>a, b, c</sup>, Huili GONG<sup>a, b, c</sup>, Zheng CHEN<sup>a, b, c</sup>, Xinming TANG<sup>d</sup>

<sup>a</sup> Key Laboratory of 3D Information Acquisition and Application of Ministry of Education, Beijing 100048, China – (b-19890320@163.com, zhwenji1215@163.com, gongzhn@163.com, gonghl@263.net, lubyn@126.com)

<sup>b</sup> Key Laboratory of Resources Environment and GIS of Beijing Municipal, Beijing 100048, China

<sup>c</sup> College of Resource Environment and Tourism, Capital Normal University, Beijing 100048, China

<sup>d</sup> Satellite Surveying and Mapping Application Center, NASG., Beijing 101300, China – (txm@sasmac.cn)

## Commission VI, WG VI/4

**ABSTRACT:** In this paper, the authors rectified ZY-3 satellite data with a total of 5 commonly used topographic correction models, and investigate its impact on the regression fitting estimation of shrub forest leaf biomass in the study area. Through visual inspection, statistical analysis and correlation analysis to evaluate every result of the correction models, and the result shows that Minnaert +SCS model based on the non-lambertian reflection assumption is supposed to be the most befitting correction for the ZY-3 image in the study area, moreover, to some extent, coefficient correlation of the biomass fitting result was improved after corrected, as well as the fitting precision. The R<sup>2</sup> reached 0.869, while the standard error dropped to 72.7 g/m<sup>2</sup>, to be specific, the coefficient correlation of the model has increased by 0.113 while the precision has improved a range of 15.8g/m<sup>2</sup>. Therefore, the authors hold the opinion that in region of large relief, topographical correction is both indispensable and essential to the estimation of the biomass based on vegetation indices.

**KEY WORDS:** Topographical correction, Non-lambertian reflection models, ZY-3 satellite, Biomass, Remote sensing estimation

## 1. INTRODUCTION

### 1.1 General Instructions

Shrub biomass is a measure of shrub community development and an important part of the study of ecological system, at the same time, biomass is the important foundation of material cycle and energy conversion, which has important research value and far-reaching significance. Actually, shrubs can grow well under drought and cold, no matter soil is rich or not, dry or wet, that makes them play a major role in water and soil conservation, as well as ecological protection and restoration. However, study of shrubs focused on the physiological and chemical characteristics (Du et al., 2011), or growth pattern (Yin et al., 2009) instead of quantitative parameters, such as biomass. Furthermore, shrub growth most in the mountains, leading to the result that canopy surface's receiving of the solar radiation energy has obvious difference, which manifest as the variance of radiation brightness value between schattenseite and adret in the same image data: the former is darker, and the latter is bright. This radiation distortion caused by the topographic relief in the remote sensing image called the topographic effect. As a result, it gives rise to different object with the same spectra characteristics, which seriously affects the quantitative inversion of vegetation parameters, as well as surface parameters.

Topographic correction refers to transform radiation brightness values (or reflectance) of all pixels to another reference plane (usually horizontal plane) from the slope in order to eliminate the terrain effect caused by topographic relief and restore the real radiation at the same time (Gao and Zhang, 2008a). Over the past 30 years, topographic correction method has been suggested and developed by numerous pioneer work. Early in

1980s, Teillet et al. (1980) put forward the Cosine model based on the assumption of a single band bidirectional reflectance parameters, then improved it to a new algorithm, which known as C correction model (Gao and Zhang, 2008b). However, because of the defects of assumption based on lambertian reflection, seriously excessive correction appears after correction. Then Huang Wei et al. (2005) further developed an improved C correction method, which simplified the calculating process on the premise of guarantee the correction effect. Afterwards, Gu and Gillespie (1998) proposed the SCS (Sun-Canopy-Sensor) model from the view of the relationship between vegetation canopy and sun radiation, which was improved by introducing regulation parameter C and named SCS+C model (Soenen et al., 2005). In view of defects of lambertian reflection theory, by introducing experience constant k, Smith (1980) proposed the distinguish Minnaert model based on the non-lambertian reflection theory, consequently solved the problem of excessive correction. Before long, Reeder (2002) simplified parameters of Minnaert model, and introduced the principle of SCS algorithm into Minnaert+SCS correction model. More recent studies by Stijn and Emilio (2011) compared the different topographic correction results on multitemporal Landsat ETM + data, the statistical results showed that for a single image, C correction model and Minnaert model is ideal, while for multitemporal data, a comprehensive C correction model is better. Shi Di et al. (2009) put forward a new topographic correction model by introducing the concept of radiation scaling factor. Combined with the lookup Table established by the 6S atmospheric correction model, the new model need only the sun azimuth parameters and atmospheric model as an input parameter, which simplified the physical model effectively. With the wide application of remote sensing in the field of ecological environment, how to improve the accuracy of quantitative analysis of remote sensing

\*Corresponding author. Tel.: +86 6890 3052.

E-mail addresses: [b-19890320@163.com](mailto:b-19890320@163.com)

is the key of the earth's surface and vegetation parameters inversion, as well as other critical problem facing all the quantitative remote sensing research. Therefore, such as geometric correction, topographic correction, atmospheric correction and many other processing is especially important. In this paper, on the basis of previous studies, the authors took Beijing JunDouShan Mountainous as study area, compared five different topographic correction result of ZY-3 multi-spectral data. Then analyzed the different effects every correction model had on the estimation of shrub leaf biomass, in order to provide dependable reference for the subsequent mountain shrub vegetation biomass inversion study on the selection of topographic correction method.

## 2. MATERIAL AND METHODS

### 2.1 Study area

The study area is located in the north of Jundu Mountain in Beijing, consisting of north of Changpin county, northeast of Yanqing county, mid-south of Huairou county and west of Miyun county (Figure 1). It has an average altitude of 587m, ranging from 182 to 1503m, and the maximum and mean slope calculated from DEM are  $76.2^\circ$  and  $22.8^\circ$ . The climate belongs to temperate semi-humid continental monsoon climate, where annual average temperature is about  $2\sim 11^\circ\text{C}$  and mean annual precipitation is 450~660 mm, and both of them change relationally with altitude. Due to the special geographical and environment condition, shrubs widely distributed in this area. Moreover, deciduous broadleaved forest and temperate coniferous forest are the main types of forest vegetation in this area, such as *Quercus*, *Tilia*, *Fraxinus*, *Acer*, *Populus*, *Pinustabulaeformis*, *Biota orientalis*. The main shrub types are *Vitexnegundo*, *Spiraeatrilobata*, *Myrpnoidsioica* and *Deutzia grandiflora*. In this area, multiple dominant species distribution are usually mixed, for example, *Vitexnegundo* mixed with wild Jujube, *Vitexnegundo* mixed with *Spiraeatrilobata* and *Prunus armeniaca*, *Vitexnegundo* mixed with *Spiraeatrilobata* and *Myrpnoidsioica* et al.

### 2.2 Data require and processing

#### 2.2.1 Image data and DEM

The ZY-3 image data used in this study acquired on 22 Aug, 2012. The solar zenith angle is  $29.58^\circ$  and solar azimuth angle is  $147.80^\circ$ . The ZY-3 satellite is at an altitude of 506km and has the sun synchronous round orbit, with a global coverage every 3~5days. There are 4 cameras boarded on ZY-3 platform, including a 2.1m resolution right view panchromatic TDI CCD camera and a pair of 3.5m resolution front and back sight panchromatic CCD camera and one 5.8 resolution right view multi-spectrum CCD camera. The multi-spectrum camera has 4 bands in the spectrum of blue ( $0.45\sim 0.52\mu\text{m}$ ), green ( $0.52\sim 0.59\mu\text{m}$ ), red ( $0.63\sim 0.69\mu\text{m}$ ) and near-infrared ( $0.77\sim 0.89\mu\text{m}$ ). It is significant to popularize application research fields by completely mined the advantages of satellites products of China in this research.

Compared with other resource satellites, ZY-3 has higher spatial resolution, higher geometric accuracy and positioning accuracy. In addition, it has side swing function and stereo mapping ability at 1:50000 scale. The experiments in this research suggested that DSM (Digital Surface Model) could be extracted from the front and back sight of high resolution panchromatic data, then through geometric correction with

1:50000 relief map and resample, DEM could be produced to the spatial resolution of 10 meters.

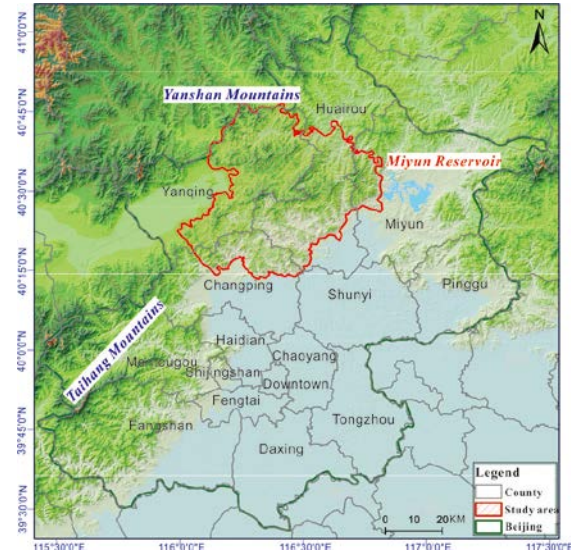


Figure 1. Location of study area schematic plot

#### 2.2.2 Field sampling data

The field investigation is a part of the National Remote Sensing Investigation and Evaluation of the Ecological Environment Changes in Ten Years (2004-2014) carried on June, 2012. During the about 3 months, 1206 points were checked and more than 300 samples were collected, which covered all over Beijing and concentrated in the northern mountains. And the field investigation in the study area is carried on August. According to geographical distribution of the shrub and the area characters, altitude and shrub types, the authors reconcile the sample area to pixel size, there are thirty  $100\text{m}\times 100\text{m}$  sample plots, and three  $30\text{m}\times 30\text{m}$  regions in every area, in which set three  $10\text{m}\times 10\text{m}$  small quadrats. Because of the limit of terrain and weather condition, we acquired 84 effective group samples in all of 90 sample regions.

In a quadrat, the dominant species, plant number was recorded and canopy leaves was weighted after cut. The record included the No. of quadrat, the GPS coordinate in the center of quadrat, altitude, slope, aspect, the name and count of dominant species, fresh weight, plant height, as well as density, and the LAI (Leaf Area Index) value and fisheye photos was marked, then the authors fetched 100g samples from every sample region into numbered bags and dried them under constant temperate in laboratory and computed values of moisture content according to expression (1), translated fresh weight to dry weight and record it. The average dry biomass of unit area ( $1\text{m}\times 1\text{m}$ ) in the sample area was recorded, of which unit is  $\text{g}/\text{m}^2$ .

$$W_i = \frac{1}{3} \sum_{j=1}^3 \left( \frac{w_{ij} \times n_{ij}}{100} \times (1 - \mu_i) \right) \quad (i = 1, 2, \dots, 72; j = 1, 2, 3;)$$

where

$w_{ij}$  = the fresh weight of the  $j$ th quadrat  
 $n_{ij}$  = the plant count of the  $j$ th quadrat  
 $\mu_i$  = the moisture content of the  $i$ th area

$W_i$  =the dry biomass of per unit area in the  $i$ th area

### 2.2.3 Data progressing

There are three steps in the processing of the satellite image: radiometric calibration, geometric correction and atmospheric correction. Firstly, according to absolute radiometric calibration parameters of ZY-3 (provided by [Satellite Surveying and Mapping Application Center, NASG.](#)), the radiometric calibration was carried on to translate DN (Digital Number) of each band to apparent radiation brightness. Secondly, the MODTRAN4 was used to correct atmospheric to calculate the reflectance. Finally, according to the RPC file and ground control points to implement ortho-rectification, of which the error was limited within 0.5 pixels. Finally, extracting the study area from the image by subimage tool in ENVI. Moreover, slope and aspect data was extracted from DEM data by modeling.

In order to ensure the effectiveness of fitting result and accuracy assessment result, the sample data was classified through stratified sampling method according to altitude. Ultimately, there were 72 groups sample data used to matching biomass model, and the remaining 12 groups used to assess the model accuracy.

## 2.3 METHODS

### 2.3.1 Topographic correction models

In present, there are four mainly types topographic correction models based on DEM mentioned in many researches. Including empirical-statistical models ([Teillet, 1982; Vincini et al., 2002](#)), normalization models ([Civco, 1989](#)), lambertian reflection models ([Dymond and Shepherd, 1999](#)) and non-lambertian reflection models ([Smith et al.,1980; Ekstrand, 1996](#)). Some common lambertian and non-lambertian reflection models are listed in Table 1.

	Topographic correction models	Expression	Present er
1	Cosine	$L_m = L \cdot (\cos \theta_s / \cos i)$	<a href="#">Teillet (1980)</a>
2	C-HuangWei	$L_m = (L - L_{\min}) \cdot \left( \frac{\cos \theta_s - \cos i_{\min}}{\cos i - \cos i_{\min}} \right) + L_{\min}$	<a href="#">Huang Wei et al. (2005)</a>
3	SCS+C	$L_m = L \cdot \left( \frac{\cos \theta_s \cdot \cos S + C}{\cos i + C} \right)$	<a href="#">Soenen et al. (2005)</a>
4	Minnaert	$L_m = L \cdot \left( \frac{\cos e}{\cos^k i \cdot \cos^k e} \right)$	<a href="#">Smith et al. (1980)</a>
5	Minnaert+S CS	$L_m = L \cdot \left( \frac{\cos^k \theta_s \cdot \cos S}{\cos^k i} \right)$	<a href="#">Reeder (2002)</a>

Table1. Topographic correction models used in these studies

where  $L_m$  = radiance after correction  
 $L$  = radiance before correction  
 $L_{\min}$  = the minimum radiance before correction  
 $\theta_s$  = the solar zenith angle  
 $S$  = the slope  
 $i$  = solar incident angle

$e$  = angle of incidence the sensor accept received, and in this paper,  $e$  valued equal to  $S$  due to the satellite angle of tilt  
 $C$  = empirical constant  
 $k$  = the Minnaert constant.

Unless otherwise specified in this paper, the meaning of each parameter here is the reference.

And the cosi can be expressed as:

$$\cos i = \cos \theta_s \cos S + \sin \theta_s \sin S \cos(\varphi_s - A) \quad (2)$$

where  $\varphi_s$  = the solar azimuth angle  
 $A$  is the aspect

In the C correction model and SCS+C model, the  $C$  can be calculate according to the linear relation between reflectance before topographical correction and cosine incident angle. The linear relation is expressed as:

$$\rho = a + b \cos i \quad (3)$$

The factor  $a$  values intercept of the linear expression while  $b$  is the ratio of the linear expression.  $C$  can be calculated by fitting result of  $a$  and  $b$ , which is express as:  $C = a/b$ .

Minnaert model is more excellent than other topographical correction models ([Law and Nichol, 2004](#)), which is based on non-lambertian reflectance assumption. It overcomes shortcomings of lambertian reflection models by adjusting the magnitude of the topographic correction through considering experience function constant  $k$ , based on the bidirectional reflectance distribution function. And Minnaert correction model is effective to correction of low topographical relief.  $K$  is a Minnaert constant which has been used to abate the magnitude of topographical correction, since came up by Minnaert in 1941. The  $k$  values range from 0 to 1 according to the surface of the object. If the surface is a lambertian,  $k$  valued 1, otherwise  $k$  valued less than 1. While the value of  $k$  relays on the type of land cover and image band, and computed by the common regression fitting linear equation.

The expression of Minnaert model in [Table1](#) can be translated as below:

$$L_m \cdot (\cos^k i \cdot \cos^k e) = L \cdot \cos e \quad (4)$$

Take logarithm on both sides, expression (4) can be translated as:

$$\ln L_m + k \ln (\cos i \cdot \cos e) = \ln (L \cdot \cos e) \quad (5)$$

Consider  $x = \ln(\cos i \cdot \cos e)$ ,  $y = \ln(L \cdot \cos e)$ ,  $m = \ln L_m$ , then we propose the linear representation of (5) as:

$$y = kx + m \quad (6)$$

One thing to note here is that, sample points are used to regression fitting must be the same type of land cover and then we can compute the value of x and y of every sample. To the sample pixel, both k and m are constants, and k can be computed by linear fitting.

Before correct topographical radiation, parameters of each model must be calculated. 5000 vegetation sample points are created randomly in each remote sensing image. C and k of every image band can be linear fitted by expression (3) and (5). In order to comparison, in this paper, The authors selected 5 common topographical correction models listed in Table 1. Then all constants value of every band are listed in Table 2.

Parameters	Band1	Band2	Band3	Band4
C	1.4144	0.6041	0.631 4	0.440 5
k(Minnaert)	0.3956	0.5620	0.551 8	0.619 6
k(Minnaert+SCS)	0.4281	0.6348	0.622 3	0.706 1

Table 2. Parameters of correction models for ZY-3 multispectral bands

### 2.3.2 Biomass estimation

In this paper, multiple regression fitting is the method to estimate biomass. The authors abstract shrub canopy biomass as a phenomenon and vegetation indices as impact factor, so that their quantitative relation could be explained by a regression model. The pioneer research suggested that correlativity exists between dry biomass of growth state vegetation and various vegetation indices (Gao et al., 2013; Li et al., 2006; Li et al., 2011; Guo et al., 2010), and it is significant to consider overall multiple vegetation indices combinations to estimate biomass.

The vegetation information of remote sensing image is expressed mainly by the spectrum characteristic and variation difference of green vegetation leaves and canopy. The correlations between vegetation information of spectrum bands and various factors or certain characteristic state are different. So, any time to establish a remote sensing biomass equation, selection of suitable remote sensing indicates factors for certain region and certain season seems very important to the result. In this paper, considering the distribution and stereochemical architecture of shrub community characteristics, the vegetation indices are impressionable to soil environment, the authors tried ten vegetation indices, including NDVI (Normalized Difference Vegetation Index)、MSAVI (Modified Soil Adjusted Vegetation Index)、GNDVI (Green Normalized Difference Vegetation Index)、MTVI2(Modified Triangular Vegetation Index 2)、MSR(Modified Simple Ratio Vegetation Index)、RDVI(Ratio Difference Vegetation Index)、IPVI(Infrared Percentage Vegetation Index)、OSAVI(Optimized Soil Adjusted Vegetation Index)、NLI(Non-Linear Index)、TVI (Triangular Vegetation Index) listed in Table 3 to fit inversion models.

Vegetation index	Full name*	Expression	Presenter
NDVI	Normalized Difference Vegetation Index	$(R_{nir} - R_{red}) / (R_{nir} + R_{red})$	Rouse et al.(1974)
MSAVI	Modified Soil Adjusted Vegetation Index	$\frac{[2R_{nir} + 1 - \sqrt{(2R_{nir} + 1)^2 - 8(R_{nir} - R_{red})}]}{2}$	Qi et al.(1994)
GNDVI	Green Normalized Difference Vegetation Index	$(R_{nir} - R_{green}) / (R_{nir} + R_{green})$	Gitelson et al.(1996)
MTVI2	Modified Triangular Vegetation Index 2	$\frac{1.5[1.2(R_{nir} - R_{green}) - 2.5(R_{red} - R_{green})]}{\sqrt{2(R_{nir} + 1)^2 - (6R_{nir} - 5\sqrt{R_{red}}) - 0.5}}$	Haboudane(2004)
MSR	Modified Simple Ratio Vegetation Index	$\frac{R_{nir}/R_{red} - 1}{\sqrt{R_{nir}/R_{red} + 1}}$	Chen et al.(1996)
RDVI	Ratio Difference Vegetation Index	$(R_{nir} - R_{red}) / \sqrt{R_{nir} + R_{red}}$	Rougean et al.(1995)
IPVI	Infrared Percentage Vegetation Index	$R_{nir} / (R_{nir} + R_{red})$	Crippen et al.(1990)
OSAVI	Optimized Soil Adjusted Vegetation Index	$(R_{nir} - R_{red}) / (R_{nir} + R_{red} + 0.16)$	Rondeaux et al.(1996)
NLI	Non-Linear Index	$(R_{nir}^2 - R_{red}) / (R_{nir}^2 + R_{red})$	Goel et al.(1994)
TVI	Triangular Vegetation Index	$0.5[120(R_{nir} - R_{green}) - 200(R_{red} - R_{green})]$	Broge et al.(2000)

\*The abbreviation of some vegetation indexes may be different from previous ones and the vegetation index names listed in the Table are new ones coming up with presentation papers

Table3 Spectral vegetation index used in this study

Figure 2 is the total technique flowcharts of biomass estimation. There are five parts in the flow: remote sensing data preprocessing and vegetation index extraction; *Vitexnegundo* extraction; field data sampling processing; model fitting and accuracy assessment and biomass distribution mapping. The remote sensing data preprocessing includes radiometric calibration, atmospheric correction, geometric correction, image clipping and ten vegetation indexes extraction. Secondly, map

shrub synthesize vegetation mapping of Beijing in 2006, DEM data, grade data, aspect data and shrub field survey results. Finally, estimate *Vitexnegundo* vegetation index and its canopy biomass fitting models by least squares method and evaluate the models accuracy to select optimal one. In the select process, remote sensing data preprocessing, topographical correction by Minnaert+SCS model, vegetation index extraction and biomass estimation by least square are in process, respectively.

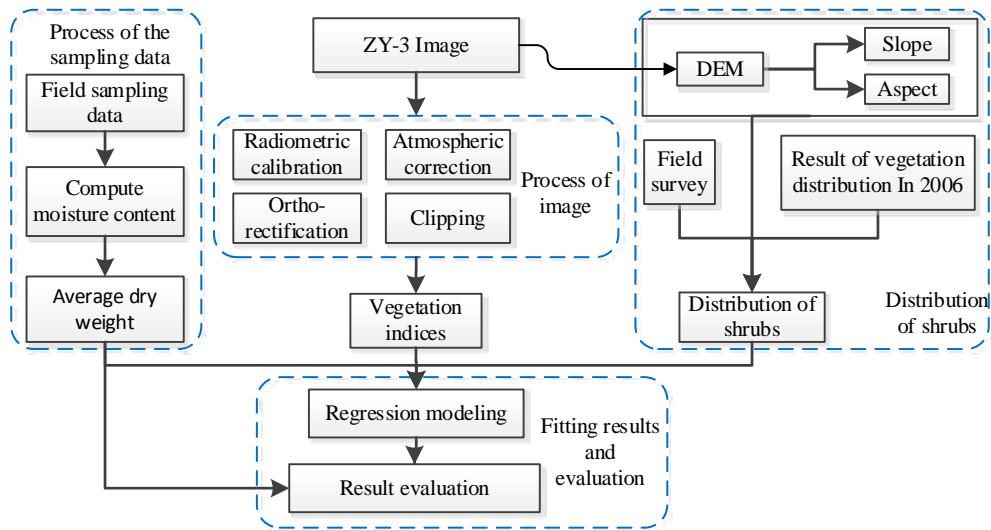


Figure 2. Total technique flowcharts of biomass estimation

### 3. RESULTS

#### 3.1 Comparison of different topographic correction models

##### 3.1.1 Visual inspection

Figure 3 shows the example of comparison before and after topographic corrections for a small area of mountainous in the study area. A clear reduction of the topographic effect can be

seen for all of these methods. The original and the results after topographic correction for the five different performing methods, the Minnaert model and Minnaert+SCS model shows the best effect. While the Cosine, C-HuangWei and the SCS+C showed similar visual effect, seriously excessive correction appeared after correction, which mainly caused by the defects of assumption based on lambertian reflection.

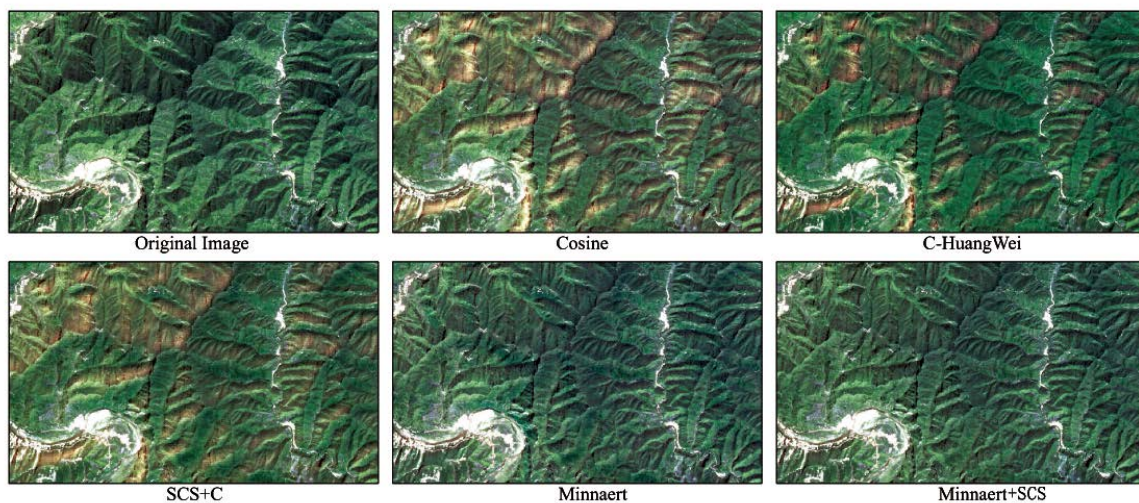


Figure 3. Comparison of results from different models

Model	Band1	Band2	Band3	Band4
-------	-------	-------	-------	-------

Name	Mean	Stdev	Mean	Stdev	Mean	Stdev	Mean	Stdev
Original Imag	0.0629	0.028	0.0918	0.039	0.0581	0.034	0.7327	0.192
Cosine	0.0633↑	0.029↑	0.0990↑	0.041↑	0.0591↑	0.035↑	0.7804↑	0.226↑
C-HuangWei	0.0625↓	0.035↑	0.0979↑	0.067↑	0.0587↑	0.040↑	0.7722↑	0.196↑
SCS+C	0.0630↑	0.033↑	0.0912↓	0.038↓	0.0553↑	0.036↑	0.7512↑	0.201↑
Minnaert	0.0628↓	0.027↓	0.0966↑	0.040↑	0.0598↑	0.034-	0.7892↑	0.185↓
Minnaert+SCS	0.0633↑	0.024↓	0.0983↑	0.038↓	0.0603↑	0.035↑	0.7504↑	0.167↓

Table4 Mean reflectance before and after topographic correction with different model for each bands

### 3.1.2 Statistical analysis

For further evaluation of the calibration results of different models, statistical comparison method is applied to make further analysis. The mean and SD (Standard Deviation) of pixel reflectance of every image band before and after correction are shown in Table 4. Mean and SD image of each band obviously increased after the Cosine and C - Huangwei correction, and the variance has increased in different level. Meanwhile the mean and SD after the SCS + C model correction presented a trend of increase, which showed that, in a sense, the three kinds of lambertian reflection model is hardly ideal in this paper. However, for Minnaert and Minnaert + SCS correction, the former is obviously better than the three, especially for Minnaert + SCS correction, of which the mean increased while the SD decreased, except for the third band. All the above showed that, Minnaert + SCS correction effect is better than the others'. Data statistics and analysis of the results confirm the results of the visual analysis again: Minnaert + SCS

model is more suitable for XY-3 multispectral image data under the condition of topography in the study area.

### 3.1.3 Correlation analysis

Pioneer study shows that pixel reflectance of image data in relief area has obviously correlation with the solar incident angle cosine at pixel' geographic coordinates, and the correlation obviously weakened or even eliminated after terrain correction (Soenen et al., 2005; Holben et al., 1980). Theoretically, the greater the slope absolute value of linear fitting expressions of the pixel reflectance and cosine, the more obvious the terrain effect; while the greater the correlation coefficient R2, the more obvious the terrain effect. Band 4, for example, by taking 5000 sample points randomly from the image before and after correction respectively, a scatter diagram (Figure 4) is shown below, the coordinate axis respectively represents pixel reflectance and the solar incident angle cosine value of the fourth band.

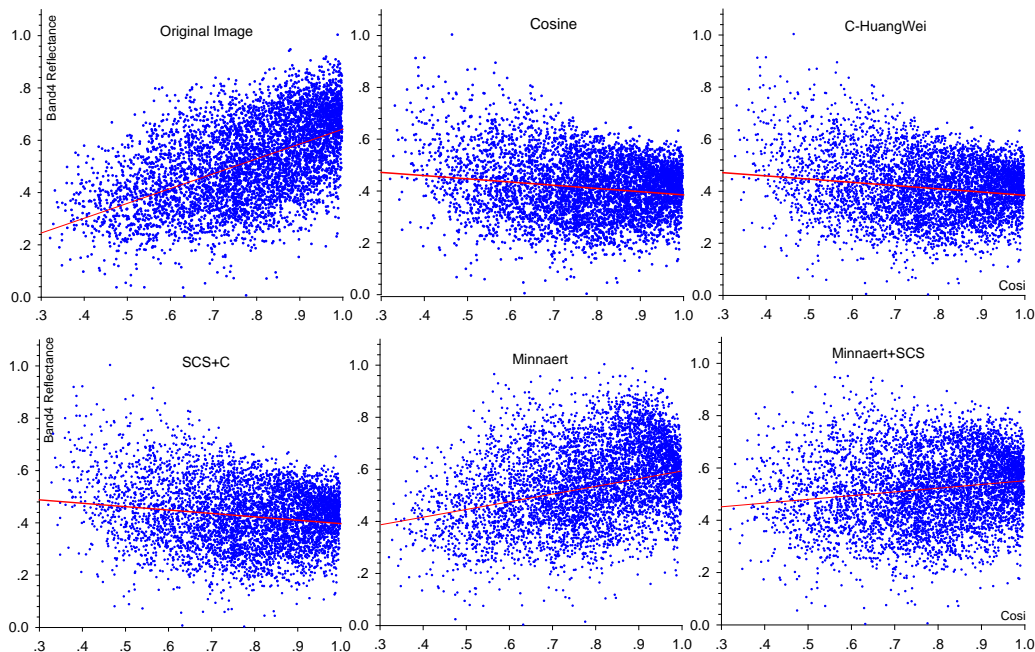


Figure 4. Scatter plots and the linear regression fitting lines of reflectance band4 and *cosi* before and after correction

As we can see from the diagram, for the original image, the scatter distribution and the regression fitting line of reflectance and *cosi* is in the tilt state obviously, while the tilt decreased significantly after correction. So it is clearly that all correction models can weaken the terrain effect in different degrees in this study. Compared with other results, to the Cosine model, C-HuangWei and SCS+C result, regression fitting lines incline to the opposite direction against the original image, due to the

excessive correction. Dissimilarly, the scatter distribution and the fitting line tilt of the Minnaert decreased significantly, as well as that of the Minnaert+SCS, which has a trend of horizontal. Furtherly, it indicates that the effect of Minnaert+SCS is better than that of Minnaert and the rest of the three models. Different pixels reflectance and *cosi* fitting results of band4 are shown in Table5. Similarly, the original image has the higher correlation coefficient (R2 reaches 0.306) and

gradient of fitting line, while Minnaert+SCS result has both of the lowest. Besides, the results of Cosine, C-HuangWei and SCS+C have a negative correlation with *cosi*. In a word, through the comparison and analysis, Minnaert + SCS correction turns out to be better effect than other models in this paper.

Correction Model	R <sup>2</sup>	Expression of fitting line
Original Image	0.306	y=0.5673x+0.0753
Cosine	0.0580	y=-0.1825x+0.5412
C-HuangWei	0.0264	y=-0.1239x+0.5086
SCS+C	0.0253	y=-0.1216x+0.5068
Minnaert	0.0263	y=0.1425x+0.4073
Minnaert+SCS	0.0246	y=0.1179x+0.4210

Table5 R<sup>2</sup> and the linear regression fitting expressions of reflectance band4 and *cosi* before and after correction

### 3.2 Effects on biomass estimation

#### 3.2.1 Fitting results of biomass

In this paper, the authors used regression analysis method to fit leaf biomass of shrub in Beijing mountain area, and solved the parameters by least square method under the premise of the minimum squares of error sum ( $\sum(\epsilon_i)^2$ ). Because of the abnormal distribution of the sample data, Kendall correlation coefficient was used in the correlation analysis between the 10 groups of vegetation indices and biomass sample data (in IBM SPSS Statistic software, version 20.0). Results showed that the NDVI, OSAVI, MTVI2, GNDVI, NLI, MSAVI, RDVI and IPVI had significant correlation with the biomass data, while TVI and MSR was not so significant; NDVI, MSAVI, GNDVI, MTVI2, MSR, RDVI and IPVI had a non-ignorable correlation with OSAVI; Meanwhile, there were significant correlation relationships between MSAVI and other vegetation index. In order to ensure the sample variables are independent and low correlation with each other, comprehensive analysis of the results, the authors removed vegetation indices that had correlation with others, such as NDVI, OSAVI and MSAVI, and chose TVI, MTVI2, GNDVI, NLI, MSR, RDVI and IPVI to fit biomass by regression method, and then got the fitting results of different terrain corrections (Table 6).

Model	Expression	R <sup>2</sup>	SE(g/m <sup>2</sup> )	Sig.	F
Original image	Y=-204.847+1209.428MTVI2-2405.185RDVI+47.623TVI+1338.759MSR+1742.851NLI+2482.307GNDVI	0.756	88.5	*	9.312
Cosine	Y=-268.452+1094.142MTVI2-1922.190RDVI+64.352TVI+1097.733MSR-1048.229NLI+1862.554GNDVI	0.787	86.4	*	8.799
C-HuangWei	Y=-229.937+1109.368MTVI2-2192.665RDVI+59.320TVI+1400.529MSR-1558.106NLI+2056.861GNDVI	0.773	84.0	*	8.752
SCS+C	Y=-238.902+1320.922MTVI2-2106.025RDVI+50.221TVI+1128.092MSR-1615.210NLI+2102.425GNDVI	0.790	82.3	*	9.017
Minnaert	Y=-302.228+1529.474MTVI2-2351.601RDVI+38.944TVI+1037.805MSR-2209.750NLI+1083.262GNDVI	0.854	76.2	**	9.362
Minnaert+SCS	Y=-217.032+1604.227MTVI2-2409.825RDVI+40.352TVI+1099.027MSR-2128.104NLI+1166.460GNDVI	.869	72.7	**	9.401

\* ANOVA is short for Analysis of Variance

\*\* Correlation is significant at the 0.01 level

\*: Correlation is significant at the 0.05 level

Table6 Model Statistics and ANOVA\*

From Table 6, the determination coefficient R<sup>2</sup> reaches more than 0.75, and the model significance is significant ( $p < 0.05$ ), which shows that the fitting models have good robustness, and they can express the quantitative relationship between vegetation indices and leaf biomass available. After the former three kind of lambertian reflection correction, fitting equation of the R<sup>2</sup> increased, but still stayed below 0.8, and have reached significant level ( $p < 0.05$ ). While for non-lambertian reflection correction, Minnaert and Minnaert + SCS, the fitting equation R<sup>2</sup> after correction reached more than 0.85, and have reached a more significant level ( $p < 0.01$ ). Furthermore, the fitting result of Minnaert + SCS correction had higher R<sup>2</sup> and precision, which increased 0.113 and 15.8 g/m<sup>2</sup> respectively in contrast to original image.

#### 3.2.2 Effects on biomass estimation

In this section, the authors used the fitting results last section for biomass estimation respectively, then the error bar diagram of estimation results and the measured biomass of the 12

samples is obtained as shown in Figure 5. At first glance, the distribution of sample bars in every diagram is near the 1:1 contour, which shows that the biomass estimation fitting results are reliable. Furthermore, for original image, inversion results with the measured SE (standard error) of 74.1 g/m<sup>2</sup>, while the error of statistics to a maximum of 99.6 g/m<sup>2</sup>, for which there are three main causes: first of all, the shrub has a special distribution and geometry architecture, mostly forested, and uneven distribution in sunny slope more than in shade; Secondly, sampling discontinuity and too much rain in August in Beijing mountain area in 2012, so that vegetation grown apace, and caused deviation of the sample data in different period; Finally, due to the geometric deformation caused by ZY-3 satellite observation angle to a certain extent, in the mountain area. In addition, the determination of regression parameters in topographic correction model is also the important factors that affect the final result. As mentioned above, the Cosine, C-HuangWei and SCS +C correction results appeared larger error in the internal where the biomass is higher

or lower, and the maximum error reached 100.2 g/m<sup>2</sup>, as a result of excessive correction in slope pixels. Meanwhile for Minnaert model and Minnaert + SCS model, based on the assumption of the lambertian reflection, showed the characteristics of stable, of

which error range are controlled within the 65 g/m<sup>2</sup>, especially for Minnaert + SCS model correction results, the SE reached a value of 58.4 g/m<sup>2</sup>, the maximum error of 64.7 g/m<sup>2</sup>.

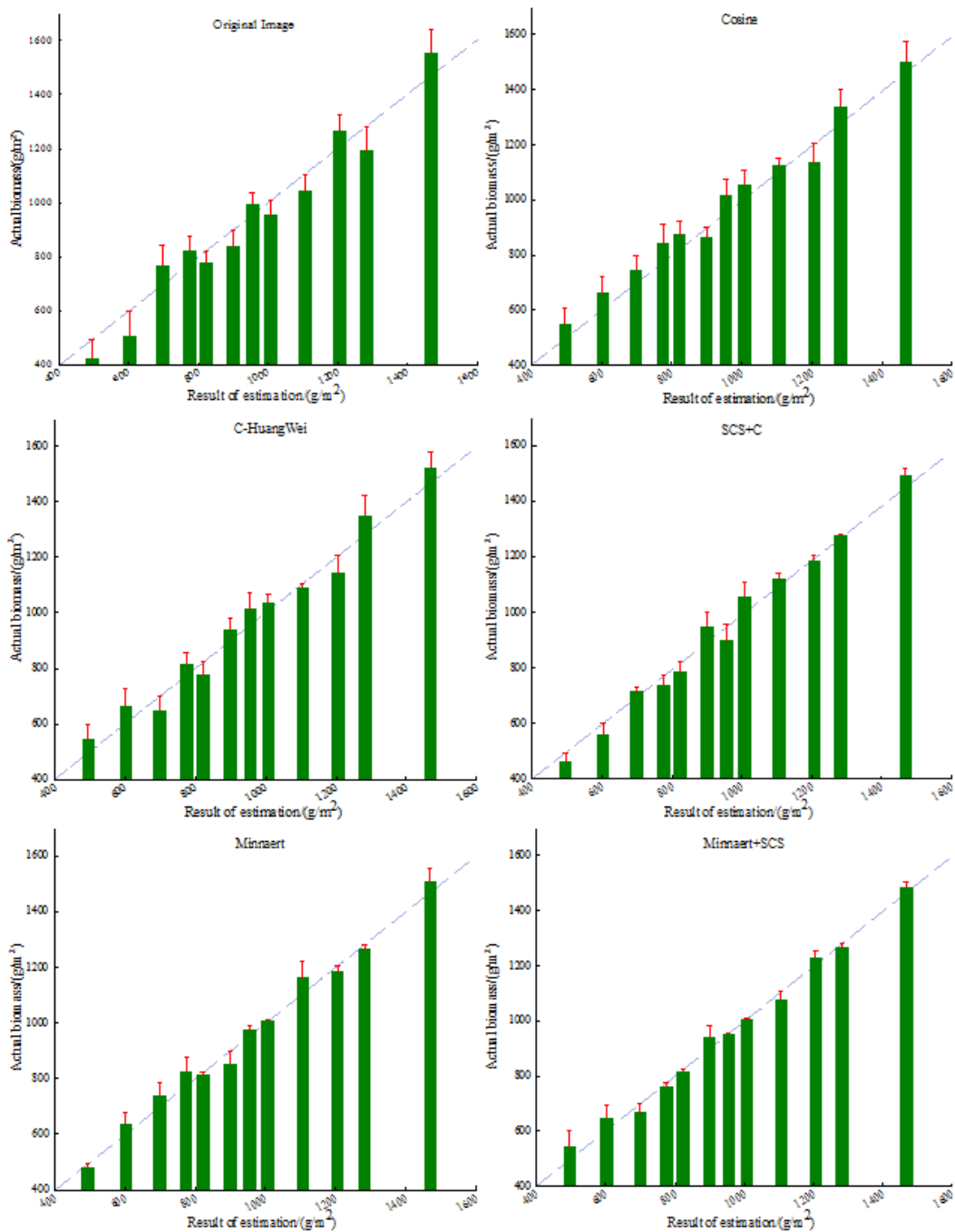


Fig.5 Comparison between predicted and actual leaf biomass

#### 4. DISCUSSION

Quantitative estimation based on remote sensing reflectance and vegetation indices, the precision of the inversion model largely depends on the basis of remote sensing data processing effect, and the determination of the parameters in the process of modeling, also, parameter selection is extremely important. In the extent of study area, the k value is a constant, while during the process of calculation, it can be found that the k partly

depends on the geometric parameters such as the solar incident angle and slope. Lu et al. (2008) found by calculation that there was a non-ignorable deviation between the fitting values of k under different slope grade, which showed that correction precision of large region of relief need to be further improved.

In this paper, in the experiment for topographic correction, the authors selected DEM resolution of 10 m, processed from ZY-3 stereopair which made up of fore sight and back sight

panchromatic images. However, it is clearly that the resolution of DEM is not consistent with that of remote sensing data, so that hardly avoid re-sampling in the process of data processing, also, it is bound to affect the precision of the topographic correction. Nevertheless, there is no definite conclusion at present about the best matching combination between the resolution of the DEM and that of the original image (Conese et al., 1993). In addition, for the topographic correction model regression parameters (such as  $k$  and  $C$ ) in the process of the calculation, the selection of random point have a fundamental impact on the results, and different sets of sample points to get the regression parameters will result in certain difference, therefore method to confirm regression parameters more scientifically also remained to be discussed. In addition, the terrain ups and downs often be associated with the change of the vertical distribution of vegetation, such as the difference of vegetation in disparate slope, and the scope of different elevation level different vegetation species in plant, and the different growth status of the same vegetation. So how to judge whether the original image pixel brightness (or reflectance) changes caused by topographic relief or characteristic spectral features itself, should be taken into consideration in the improvement of the topographic correction method.

Besides, regression model of biomass based on empirical statistical regression algorithm, which is limited to the special time and environmental conditions, as well as the processing method of field sampling data, and in different seasons and different geographical conditions, the biomass fitting result come into being a significant difference. Because of the discontinuous distribution of the shrub, combined with the special plant architecture of shrub, pixels in remote sensing image is affected by the soil background readily. Moreover, due to the resistant ability to cold and drought, shrubs also distribute in the high altitude and localities infertile area, where the reflectance of canopy is easily affected by the background of soil and rock. Therefore, how to improve the typicality of sampling and the universality of inversion model, is also in content of further research.

## 5. CONCLUSION

In this paper, the author compared the correction effects of five different common topographic correction models on the ZY-3 satellite multispectral images, then discusses the effects on shrubs biomass estimation after correction in the study area, the conclusion summarizes as follows:

- (1) The topographic correction model based on lambertian reflection theory, due to the sky diffuse reflection and the surrounding terrain, easily lead to the result of excessive correction, while for models based on the lambertian reflection assumption, the correction effect had improved significantly than the former. After the visual contrast, statistical analysis and correlation analysis, the results shows that the Minnaert + SCS model can effectively weaken the influence of terrain relief on pixels in ZY-3 satellite multispectral images, and reflectivity restore true reflection of the pixels in relief area.
- (2) Precision of regression fitting results between spectral vegetation indices and shrub leaf biomass are improved after topographic correction, as well as the determination coefficient  $R^2$ , which shows topographic correction on the ZY-3 satellite data has a certain degree of improvement to estimate shrubs leaf biomass, in addition, results based on non-lambertian reflection model is superior to these based on lambertian reflection model. Furtherly, after the correction of Minnaert + SCS model, the

biomass regression fitting result has the  $R^2$  of 0.869, and the SD is reduced to 58.4 g/m<sup>2</sup>, which suggests that in areas of topographic relief, topographic correction is indispensable to the biomass estimation based on vegetation indices.

## Acknowledgment

This research was financially supported by the National Natural Science Foundation of China (Grant No. 41101404) and National Foundation Survey Project (Grant No. 2011A2001). Thanks Prof. Hu Dong for the guidance on the field data, and the ZY-3 satellite data and related parameters are provided by Satellite Surveying and Mapping Application Center, NASG.

## References

- Broge, N. H., Leblanc, E., 2000. Comparing prediction power and stability of broadband and hyperspectral vegetation indices for estimation of green leaf area index and canopy chlorophyll density. *Remote Sensing of Environment*, 76(2), pp. 156-172.
- Chen, J., 1996. Evaluation of vegetation indices and a modified simple ratio for boreal applications. *Canadian Journal of Remote Sensing*, 22, pp. 229-242.
- Civco, D. L., 1989. Topographic normalization of landsat thematic mapper digital imagery. *Photogrammetric Engineering and Remote Sensing*, 55(9), pp. 1303-1309.
- Conese, C., Gilabert, M. A., Maselli, F., et al., 1993. Topographic normalization of TM scenes through the use of an atmospheric correction method and digital terrain models. *Photogrammetric Engineering and Remote Sensing*, 59(12), pp. 1745-17531.
- Crippen, R. E., 1990. Calculating the vegetation index faster. *Remote Sensing of Environment*, 34(1), pp. 71-73.
- Deering, D. W., Haas, R. H., Rouse, J. W., Schell, J. A., 1974. Monitoring the vernal advancement of retrogradation of natural vegetation. NASA/GSFC, Type III, Final Report. Greenbelt, MD, USA.
- Du, N., Zhang, X. R., Wang W., Chen H., Tan, X. F., Wang, R. Q., Guo, W. H., 2011. Foliar phenotypic plasticity of a warm-temperate shrub, *Vitex negundo* var. *Heterophylla*, to different light environments in the field. *Acta Ecologica Sinica*, 31(20), pp. 6049-6059.
- Dymond, J. R., Shepherd, J. D., 1999. Correction of the topographic effect in remote sensing. *IEEE Transactions on Geoscience and Remote Sensing*, 37(5), pp. 2618-2620.
- Ekstrand, S., 1996. Landsat TM-based forest damage assessment: Correction for topographic effects. *Photogrammetric Engineering and Remote Sensing*, 62(2), pp. 51-161.
- Gao, M. L., Zhao, W. J., Gong, Z. N., 2013. and He X. H., The study of vegetation biomass inversion based on the HJ satellite data in Yellow River wetland. *Acta Ecologica Sinica*, 33(2), pp. 542-553.

- Gao, Y. N., Zhang, W. C., 2008a. Comparison test and research progress of topographic correction on remotely sensed data. *Geographical Research*, 27(2), pp. 467-477.
- Gao, Y. N., Zhang, W. C., 2008b. Simplification and modification of a physical topographic correction algorithm for remotely sensed data. *Acta Geodaetica et Cartographica Sinica*, 37(1), pp. 89-94.
- Gitelson, A. A., Kaufman, Y. J., Merzlyak, M. N., 1996. Use of a green channel in remote sensing of global vegetation from EOS-MODIS. *Remote Sensing of Environment*, 58(3), pp. 289-298.
- Goel, N. S., Qin, W. H., 1994. Influences of canopy architecture on relationships between various vegetation indices and LAI and FPAR: a computer simulation. *Remote Sensing Reviews*, 10(4), pp. 309-347.
- Gu, D., Gillespie, A., 1998. Topographic normalization of landsat TM images of forest based on subpixel Sun-Canopy-Sensor geometry. *Remote Sensing of Environment*, 64(2), pp. 166-175.
- Guo, Z. F., Chi, H., Sun, G. Q., 2010. Estimating forest aboveground biomass using HJ-1 Satellite CCD and ICESat GLAS waveform data. *Science in China: Earth Sciences*, 53(1), pp. 16-25.
- Haboudane, D., Miller, J. R., Pattey, E., Zarco-Tejada, P. J., Strachan, I. B., 2004. Hyperspectral vegetation indices and novel algorithms for predicting green LAI of crop canopies: Modeling and validation in the context of precision agriculture. *Remote Sensing of Environment*, 90(3), pp. 337-352.
- Holben, B. N., Justice, C. O., 1980. The topographic effect on spectral response from Nadir-Pointing sensors. *Photogrammetric Engineering and Remote Sensing*, 46(9), pp. 1191-1200.
- Huang, W., Zhang, L. P., Li, P. X., 2005. An improved topographic correction approach for satellite image. *Journal of Image and Graphics*, 10(9), pp. 1124-1128.
- Law, K. H., Nichol, J., 2004. Topographic correction for differential illumination effects on IKONOS satellite imagery. In proceedings: *XXth congress of International Society for Photogrammetry and Remote Sensing*, Istanbul, Turkey, 35, pp. 6.
- Li, S., Zhang, Z. L., Zhou, D. M., 2011. An estimation of aboveground vegetation biomass in a national natural reserve using remote sensing. *Acta Ecologica Sinica*, 30(2), pp. 278-290.
- Li, X., Yeh A., Liu, K., Wang, S. G., 2006. Inventory of mangrove wetlands in the pearl river estuary of China using remote sensing. *Journal of Geographical Sciences*, 16(2), pp.155-164.
- Lu, D. S., Ge, H. L., He, S. Z., et al., 2008. Pixel-based Minnaert correction method for reducing topographic effects on a landsat 7 eTM+ image. *Photogrammetric Engineering & Remote Sensing*, 74(11), pp. 1343-1350.
- Qi, J., Chehbouni, A., Huete, A. R., Kerr, Y. H., Sorooshian, S., 1994. A modified soil adjusted vegetation index. *Remote Sensing of Environment*, 48(2), pp. 119-126.
- Reeder, D. H., 2002. *Topographic Correction of Satellite Images: Theory and Application*. Hanover, New Hampshire: Dartmouth College.
- Rondeaux, G., Steven, M., Baret, F., 1996 Optimization of soil-adjusted vegetation indices. *Remote Sensing of Environment*, 55(2), pp. 95-107.
- Roujean, J. L., Breon, F. M., Estimating PAR absorbed by vegetation from bidirectional reflectance measurements. *Remote Sensing of Environment*, 51(3), pp. 375-384.
- Smith, J. A., Lin, T. L., Ranson, K. J., 1980. The lambertian assumption and landsat data. *Photogrammetric Engineering and Remote Sensing*, 46(9), pp. 1183-1189.
- Soenen, S. A., Peddle, D. R., Coburn, C. A., 2005. SCS+C: A modified Sun-Canopy-Sensor topographic correction in forested terrain. *IEEE Transactions on Geoscience and Remote Sensing*, 43(9), pp. 2148-2159.
- Stijn, H., Emilio, C., 2011. Evaluation of different topographic correction methods for landsat imagery. *International Journal of Applied Earth Observation and Geoinformation*, 13, pp. 691-700.
- Tillet, P. M., Guindon, B., Goodenough, D. G., 1982. On the slope-aspect correction of multispectral scanner data. *Canadian Journal of Remote Sensing*, 8(2), pp. 1537-1540.
- Vincini, M., Reeder, D., Frazzi, E., 2002. An empirical topographic normalization method for forest TM data. *Geoscience and Remote Sensing Symposium, 2002. IGARSS'02. 2002 IEEE International. IEEE*, 2002, 4, pp. 2091~2093.
- Yang, G. J., Mu, X. H., 2009. Optical remote sensing image apparent radiance topographic correction physical model. *Journal of Remote Sensing*, 13(6), pp. 1039-1046.
- Yin, Z. F., Ouyang, H., Xu, X. L., Song, M. H., Duan, D. Y., Zhang, X. Z., 2009. Water and heat balance and water use of shrub grassland and crop fields in Lhasa River Valley. *Acta Geographica Sinica*, 64(3), pp. 303-314.